

Inorganic Nanoporous Films from Block Copolymer Thin Film

Yumei Gong,[†] Wonchul Joo, Youngsuk Kim, and Jin Kon Kim*

National Creative Research Initiative Center for Block Copolymer Self-Assembly, Department of Chemical Engineering, Pohang University of Science and Technology, Pohang, Kyungbuk 790-784, Korea

Received September 14, 2007

Revised Manuscript Received December 16, 2007

Inorganic nanoporous films have drawn much attention because of promising applications for separation membranes, optoelectronics, and photocatalysts.^{1–4} Among many methods to prepare nanoporous structure in inorganic films, block copolymers have been widely employed.^{4–11} For instance, nanoporous silica in bulk and film is easily prepared by using amphiphilic block copolymers such as poly(ethylene oxide)-*block*-poly(propylene oxide) copolymers (Pluronic),^{5–8} polystyrene-*block*-poly(ethylene oxide) copolymers,⁹ and polystyrene-*block*-poly(vinyl pyridine) copolymers.¹⁰ In this case, the precursor of silica (tetraethoxysilane, TEOS) is easily incorporated into the hydrophilic block. After a sol–gel reaction followed by calcinations, a well-defined nanoporous structure is obtained. Recently, nanoporous silica and titania films were obtained where the pores were oriented vertically across the entire thickness.^{6,7,12}

However, the above methods need special precursors miscible with the hydrophilic block and hence other important inorganic nanoporous film, such as zinc oxide, could not be prepared. For this purpose, templates with nanopillars should be used. Polystyrene-*block*-poly(methyl methacrylate) copolymer (PS-*b*-PMMA) has been extensively employed for the templates because the PMMA component is easily removed by UV irradiation followed by rinsing with acetic

acid.^{13–17} Almost all the reports showed a vertical orientation of minor PMMA block and accordingly the templates exhibit cylindrical nanoporous structure. By using this kind of template, one can only prepare inorganic nanodots or metal nanowires.^{13–15} Therefore, to develop a universal approach to nanoporous inorganic film, one should have a vertical orientation of minor PS block in the PMMA matrix. Although only a few studies have reported that vertical PS cylindrical microdomains could be achieved on a silicon wafer modified by an energetically neutral brush,^{16,17} the achievable maximum height (~ 30 nm) is too small to be used for photovoltaic devices with high power conversion efficiency that needs a thicker inorganic film (say, ~ 100 nm) having vertically oriented cylindrical nanopores.²

In this study, we obtained cylindrical PS microdomains oriented vertically to a substrate in PS-*b*-PMMA film with a thickness of ~ 100 nm by using solvent vapor annealing after thermal annealing at a high temperature. After removing PMMA chains, the film has PS nanopillar structure. Because of this unique nanopillar structures, a wide range of inorganic films with vertical orientation of cylindrical pores spanning the entire film thickness could be easily prepared. For instance, nanoporous zinc oxide film is easily prepared by this template, which could not be prepared by amphiphilic block copolymer template that has been widely used for the preparation of nanoporous silica or titania.

We describe briefly the preparation of inorganic nanoporous films (details are given in the Supporting Information). A PS-*b*-PMMA with a volume fraction of PS of 0.27 was spin-coated onto a silicon wafer modified by a neutral brush and annealed at high temperature. Then, the film was annealed under acetone vapor to have vertically oriented cylindrical microdomains of PS block. After the PMMA matrix was removed by UV irradiation and selective rinsing, inorganic films were prepared through chemical solution method for zinc oxide or sol–gel chemistry for titania and silica. Finally, the PS nanopillars in the film were removed by thermal decomposition at high temperature, generating inorganic nanoporous films.

Figure 1 shows the typical morphology of the block copolymer thin film after thermal annealing at 230 °C for 5 h. Figure 1a shows scanning probe microscopy (SPM) phase image of the thermally annealed PS-*b*-PMMA film. Because the PMMA block is harder than PS block at room

* To whom correspondence should be addressed. E-mail: jkkim@postech.ac.kr.

[†] Present address: School of Chemical Engineering and Materials, Dalian Polytechnic University, Dalian 116034, P. R. China.

- (1) Pal, B.; Sharon, M. *Mater. Chem. Phys.* **2002**, *76*, 82–87.
- (2) Coakley, K. M.; McGehee, M. D. *Chem. Mater.* **2004**, *16*, 4533–4542.
- (3) Zhang, X.; Sato, O.; Taguchi, M.; Einaga, Y.; Murakami, T.; Fujishima, A. *Chem. Mater.* **2005**, *17*, 696–700.
- (4) Malenfant, P. R. L.; Wan, J.; Taylor, S. T.; Manoharan, M. *Nat. Nanotechnol.* **2007**, *2*, 43–46.
- (5) Coakley, K. M.; Liu, Y.; McGehee, M. D.; Frindell, K. L.; Stucky, G. D. *Adv. Funct. Mater.* **2003**, *13*, 301–306.
- (6) Koganti, V. R.; Rankin, S. E. *J. Phys. Chem. B* **2005**, *109*, 3279–3283.
- (7) Koganti, V. R.; Dunphy, D.; Gowrishankar, V.; McGehee, M. D.; Li, X.; Wang, J.; Rankin, S. E. *Nano Lett.* **2006**, *6*, 2567–2570.
- (8) Fattakhova-Rohlfing, D.; Wark, M.; Brezesinski, T.; Smarsly, B. M.; Rathousky, J. *Adv. Funct. Mater.* **2007**, *17*, 123–132.
- (9) Freer, E. M.; Krupp, L. E.; Hinsberg, W. D.; Rice, P. M.; Hedrick, J. L.; Cha, J. N.; Miller, R. D.; Kim, H. C. *Nano Lett.* **2005**, *5*, 2014–2018.
- (10) Cha, J. N.; Zhang, Y.; Philip Wong, H. S.; Raoux, S.; Rettner, C.; Krupp, L.; Deline, V. *Chem. Mater.* **2007**, *19*, 839–843.
- (11) Cheng, Y. J.; Müller-Buschbaum, P.; Gutmann, J. S. *Small* **2007**, *3*, 1379–1382.
- (12) Walcarius, A.; Sibottier, E.; Etienne, M.; Chanabaja, J. *Nat. Mater.* **2007**, *6*, 602–608.

- (13) Thurn-Albrecht, T.; Schotter, J.; Kastle, C. A.; Emley, N.; Shibauchi, T.; Krusin-Elbaum, L.; Guarini, K.; Tuominen, M. T.; Russell, T. P. *Science* **2000**, *290*, 2126–2129.
- (14) Kim, H. C.; Jia, X.; Stafford, C. M.; Kim, D. H.; McCarthy, T. J.; Tuominen, M. T.; Hawker, C. J.; Russell, T. P. *Adv. Mater.* **2001**, *13*, 795–797.
- (15) Guarini, K. W.; Black, C. T.; Yeung, S. H. I. *Adv. Mater.* **2002**, *14*, 1290–1294.
- (16) Shin, K.; Leach, K. A.; Goldbach, J. T.; Kim, D. H.; Jho, J. Y.; Tuominen, M.; Hawker, C. J.; Russell, T. P. *Nano Lett.* **2002**, *2*, 933–936.
- (17) Zschech, D.; Kim, D. H.; Milenin, A. P.; Scholz, R.; Hillebrand, R.; Hawker, C. J.; Russell, T. P.; Steinhart, M.; Gösele, U. *Nano Lett.* **2007**, *7*, 1516–1520.

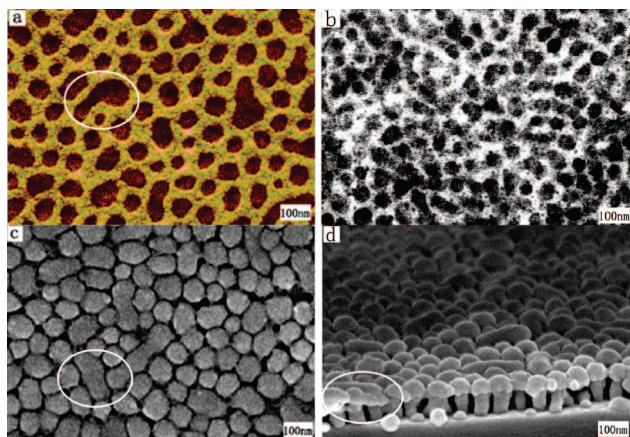


Figure 1. Morphology of the thermally annealed PS-*b*-PMMA film (a) SPM phase contrast image and (b) TEM image of the film before the removal of PMMA. (c) Plane-view and (d) cross-sectional FE-SEM images of the film after the removal of PMMA matrix. The white circles in parts a and c, looking like parallel PS microdomains at the film surface, become the mushroom caps (white circle in part d).

temperature, the PMMA phase looks brighter in an SPM phase image.^{18,19}

Therefore, the dispersed phase looking darker in the SPM phase image should be PS phase, and the volume fraction of the PS microdomains (with sizes ranging from 43 to 200 nm) at the film surface is calculated to be 0.46, much larger than that (0.27) in the bulk. The increased amount of PS at the surface of the film compared with in bulk is attributed to the comparatively lower surface tension of PS. The surface tensions of PS and PMMA are 40.7 mJ/m² and 41.1 mJ/m², respectively.^{20,21} Figure 1b shows TEM image of this film, where PS microdomains appearing darker because of selective staining are seen as dispersed phase, which is consistent with SPM phase contrast image.

Images c and d in Figure 1 give plane-view and cross-sectional FE-SEM images of the film, respectively, after PMMA matrix is removed. Vertical mushroom-shaped PS cylinders consisting of larger sized cap and smaller sized stem are observed. Mushroom caps marked by the white circles in Figure 1d are formed from the short parallel PS microdomains at the film surface (see also the circles in images a and c in Figure 1). Therefore, we consider that the vertical PS cylinders in the original film are not straight but mushroom-shaped. The formation of this interesting morphology is attributed to the film thickness and thermal annealing at a high temperature (230 °C). We found that when the film was annealed at lower temperature (say, 180 °C), we could not obtain the vertically oriented mushroom-shaped morphology, but most PS cylinders are oriented parallel to the substrate. Previously, the vertical PS cylinders were achieved in a film thickness with about one period of the domain spacing (30 nm), when a neutral brush was used.^{16,17}

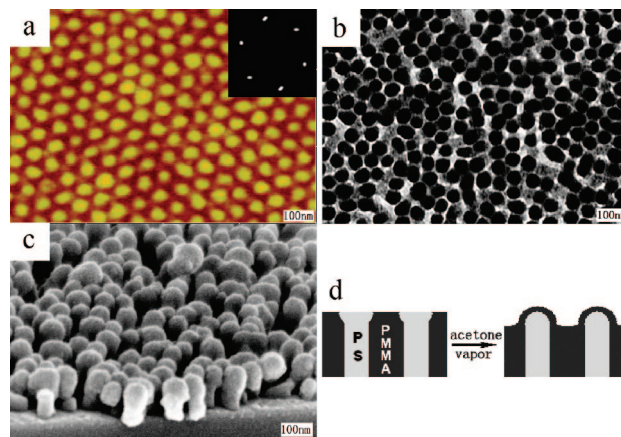


Figure 2. Morphology of the PS-*b*-PMMA film after acetone vapor annealing for 20 h at room temperature. (a) SPM height image and (b) TEM image before the removal of PMMA. (c) Cross-sectional SEM image of the film after the removal of PMMA matrix. (d) Schematic of the formation of the straight PS cylinders by acetone vapor treatment: left, the original film with mushroom-shaped PS cylinders vertically oriented to the surface; right, after acetone vapor anneal, straight PS cylinders oriented vertically on a substrate have been obtained.

For a higher thickness (~ 110 nm) of PS-*b*-PMMA film, which is larger than one period of the domain spacing of 66 nm, the PS chains have a tendency to cover more the surface of the film compared with PMMA chains during thermal annealing at high temperature because of lower surface tension. Since the surface tension difference between PS and PMMA decreases with increasing temperature,^{20,21} the PMMA component would have more chance to be located at the film surface when the film is annealed at a high temperature. Nevertheless, high temperature cannot mediate the surface tension completely; thus PS still prefers to locate at the film surface. Namely, the content of PS phase at the film surface is higher than that in film bulk.

Even though this interesting mushroom-shaped structure could be employed as a template, it is not useful to make inorganic nanoporous films with straight cylindrical pores. Thus, to develop straight PS cylinders from the above mushroom-shaped PS cylinders, in this study we employed solvent annealing of the film with acetone vapor, a selective good solvent for PMMA.^{18,19} Figure 2a gives SPM height image of PS-*b*-PMMA film after annealing under acetone vapor for 20 h at room temperature. Hexagonally ordered dispersed PS domains, confirmed by the six sharp first order peaks in the FFT image (the inset of Figure 2a), are formed, indicating that PS cylinders are oriented normal to the substrate. Interestingly, the height of the PMMA matrix is lower than PS cylinders, which is different from SPM image of the film without solvent annealing where the PS phase is higher than PMMA phase. This is explained as follows. For a solvent-annealed film, the solvent content in PMMA microdomains is higher than that in PS microdomains due to the selective solvent to PMMA chains. After drying, the shrinkage of PMMA blocks would be greater than that of PS block, leaving depressed PMMA continuous phases at the film surface. This is also confirmed by the TEM image given in Figure 2b that the size of PS pillars looking dark is similar to the protrusion part (PS phase) in Figure 2a.

(18) *Polymer Handbook*, 3rd ed.; Brandrup, J., Immergut, E. H., Eds.; John Wiley & Sons: New York, 1989.

(19) *Properties of Polymers*; Van Krevelen, D. W. Elsevier Scientific: New York, 1976.

(20) Wu, S. *Polymer Interface and Adhesion*; Marcel Dekker Inc.: New York, 1982.

(21) Mansky, P.; Russell, T. P.; Hawker, C. J.; Mays, J.; Cook, D. C.; Satija, S. K. *Phys. Rev. Lett.* **1997**, 79, 237–240.

Figure 2c gives cross-sectional FE-SEM image after PMMA is removed. Well-ordered vertical PS cylinders with a diameter of ~ 40 nm were obtained. From the above results, we conclude that acetone vapor is an effective means for modifying the mushroom-shaped PS cylinders in the original film to the straight PS cylinders. This process is schematically shown in Figure 2d. When the film is exposed to acetone vapor, acetone can easily penetrate into the film and can increase the mobility of both components and finally reconstruct both chains to minimize the free energy of the film. Because acetone has a stronger tendency to attract PMMA chains than PS chains to maximize PMMA and solvent contacts, PMMA chains must be pulled toward the film surface. Eventually, the PMMA migrates to the film surface and covers it. This was confirmed by the water contact angle of the film after the solvent annealing having $\sim 68^\circ$, identical to that of PMMA homopolymer. It is noted that the thermal annealed film without acetone vapor annealing has a contact angle of 79° , due to the existence of both PS and PMMA chains at the surface. When PMMA chains cover the film surface, the size of the mushroom cap is decreased to reduce the interfacial tension between PS and PMMA, but the inside film structure is not changed much because of the effect of the neutral brush.

The acquired film with vertically oriented PS pillars can be used as a template for inorganic films with cylindrical nanopores. In this study, three different inorganic nanoporous films (ZnO, TiO₂, and SiO₂) have been prepared. Details for the preparation of inorganic nanoporous films are described in the Supporting Information. It is noted that an attention should be paid to removing the excess precursors adsorbed at the template surface. Otherwise, one cannot obtain inorganic films with vertically aligned pore spanning through the entire thickness. This is a very important requirement for the use of nanoporous templates as functional membranes.

Figure 3 gives plane-view and cross-sectional FE-SEM images of ZnO (images a and b in Figure 3), TiO₂ (images c and d in Figure 3), and SiO₂ (images e and f in Figure 3), respectively, after removal of the PS nanopillars by thermal decomposition at high temperature. It shows that straight cylindrical pores spanning the entire film thickness were observed for all of the inorganic films. Also, the asymmetric (not circular) pores are hexagonally packed, although not perfect, because the six spots in the FFT images in each plane-view FE-SEM are observed. This indicates that the interdistance of two neighboring PS nanopillars, which becomes the distance between the pores, is maintained even after inorganic nanoporous film is prepared. However, the sizes of the pores of the three materials are different. Namely, the average diameter of the asymmetric pores of ZnO, TiO₂, and SiO₂ films are 26 ± 5 , 21 ± 7 , and 32 ± 5 nm, respectively, suggesting that the three materials have different shrinkage. Moreover, the pore diameters of all three materials are smaller than that (~ 40 nm) of PS pillar. Also, the film thickness of all three materials was ~ 80 nm, which is smaller than that (~ 110 nm) of the original PS nanopillar film, and the pores are not symmetric. This is attributed to the fact

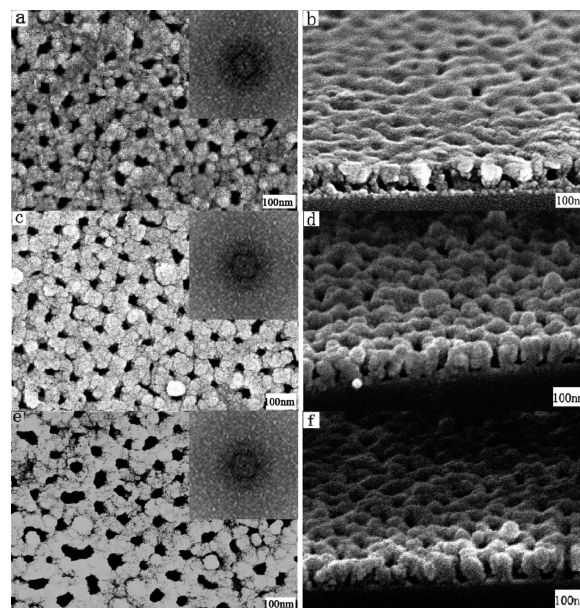


Figure 3. Morphologies of the inorganic nanoporous films prepared by using the PS nanopillar film as a template. Plane-view (a, c, e) and cross-sectional (b, d, f) FE-SEM images of nanoporous ZnO (a, b), TiO₂ (c, d), and SiO₂ (e, f) films. Fast Fourier transform (FFT) of the plane-view FE-SEM is shown as the inset of each figure.

that most of the shrinkage occurs in the direction normal to the substrate during calcinations at high temperature, as reported in ref 5.

In summary, we show a method for preparing inorganic nanoporous films by using the template with PS nanopillars oriented vertically to a substrate. This nanopillar structure was prepared by thermal annealing and subsequent solvent vapor annealing of PS-*b*-PMMA film followed by removal of the PMMA matrix. This template would be very useful for preparing a wide range of inorganic nanoporous films because the precursors could be independently selected regardless of the compatibility between the precursor and one of the blocks. One interesting application for this template is to prepare nanoporous zinc oxide film that could not be prepared by amphiphilic block copolymer templates (such as Pluronic surfactants). Since nanoporous ZnO films exhibiting excellent electron donating property (N-type) are also prepared onto indium-tin-oxide coated glass, this template could be used for photovoltaic devices with high power conversion efficiency, if proper hole-donating materials (P-type) are electrodeposited or electropolymerized inside the porous ZnO films.² Because the inorganic nanoporous films exhibit good thermal and mechanical stabilities, these could be also employed for special membranes for the separation at very high temperatures.

Acknowledgment. This work was supported by the National Creative Research Initiative Program supported KOSEF.

Supporting Information Available: Experimental details (PDF). This material is available free of charge via the Internet at <http://pubs.acs.org>.

CM7026256